DOI: 10.31276/VJSTE.65(1).19-24

Development of a miniaturised potentiostat for urea detection using the LMP91000

Chi Tran Nhu, Phu Nguyen Dang*, Tung Bui Thanh, Trinh Chu Duc

University of Engineering and Technology, Vietnam National University - Hanoi, 144 Xuan Thuy Street, Cau Giay District, Hanoi, Vietnam

Received 5 September 2022; accepted 29 November 2022

Abstract:

In this report, we develop a low-cost cyclic voltammetry platform for electrochemical analyses based on the LMP91000 integrated circuit (IC). The proposed system can be suitable to detect chemicals of interest in food safety or biology. The system includes three main blocks: the electrodes, electrochemical measuring circuit, and data acquisition. An algorithm was also built to process and display the data on the screen. Experiments are carried out with a standard redox solution containing Fe(II)/Fe(III) 5 mM and KCl 0.1 mM to evaluate system performance and make comparisons to the commercial potentiostat. The results show that the obtained signals from the proposed system and the commercial potentiostat device are similar. With applications of the miniaturised potentiostat, a non-enzymatic electrochemical biosensor for urea detection was fabricated on cobalt sulphide materials (CoS) synthesized via a microwave assisted method. The sensing performance for urea was determined by changing the oxidation potential peak of 100 mV. The sensor had a linear range from 1-8 mM corresponding to the urea concentration in blood. The sensor sensitivity was comparable (7.5 $\mu AmM^{-1}cm^{-2}$) to some previous publications. With the achieved results, the proposed system demonstrates potential in urea detection and can be a prototype to develop a commercial device for point-of-care testing in the future.

Keywords: **electrochemical system, LMP91000, urea detection.**

Classification numbers: **2.2, 2.3**

1. Introduction

Electrochemical biosensors presently attract significant interest from research groups worldwide. Electrochemical biosensors are a subclass of biological sensors that includes biological sensing elements and electrochemical transducers [1]. These sensors show outstanding advantages in terms of sensitivity, low detection limits, and high specificity of biological recognition elements [2]. These recognition elements can be enzymes, antibodies, deoxyribonucleic acid or ribonucleic acid (DNA/RNA), tissues, or other biomolecules, which react selectively with the target analyte and subsequently provide an electrical signal proportional to the target analyte's concentration. The signal is converted and processed by the transducer and microcontrollers, respectively. Based on the nature of the biological sensing elements, there are two main types of electrochemical sensors: biocatalytic devices and affinity sensors [3]. While biocatalytic devices use enzymes to sense the target analyte, affinity sensors employ selective binding interactions between the analyte and a biological component. Electrochemical biosensors have been developed to detect a wide variety of analytes such as lactate [4, 5], sodium [6, 7], cocaine [8-10], alcohol [11, 12], and glucose [13, 14]. In addition, electrochemical biosensors have been used for the detection of some diseases in humans such as celiac disease [15], breast cancer [16, 17], prostate cancer [18], and the hepatitis B virus [19].

Potentiostats are a popular instrument designed to perform electrochemical measurements. They can control the working electrode's potential and have features for accurate measurements of the electrochemical cell [20]. Some commercial potentiostats used in laboratories include Sensit BT Model (PalmSens, The Netherlands), AutoLab (Metrohm, The Netherlands), and CS350 EIS Potentiostat/Galvanostat (Orrtestinstruments, China). However, these are expensive and sophisticated instruments that are difficult to apply to point-of-care applications. Presently, research groups around the world are focusing on the development of self-designed potentiostats to increase the affordability and accessibility of potentiostats as well as to miniaturize their electrochemistry hardware for at-home or portable diagnostic applications [21-24]. These potentiostats can be built from discrete electronic components or from an IC. One commonly used IC is the LMP91000 IC developed

*Corresponding author: Email: phund@vnu.edu.vn

by Texas Instruments, a programmable analogue front-end (AFE) for use in micro-power electrochemical sensing applications. The LMP91000 contains the core features of a benchtop potentiostat and is packed with a size of 4 mm × 4 mm [25]. The LMP91000 can perform some basic electrochemical techniques such as cyclic voltammetry (CV), chronoamperometry (CA), square wave voltammetry (SWV), and normal pulsed voltammetry (NPV) and has so far demonstrated its potential in some biomedical applications [25].

Urea is a waste product of living creatures and the major organic component of human urine. It is the final product of a chain of reactions that break down amino acids making up proteins. These amino acids are converted into ammonia, CO_2, water, and energy. However, ammonia is a substance that is harmful to the body, so must be eliminated. In the human body, the liver converts ammonia to urea, a non-toxic compound, which can then be safely transported in the blood to the kidneys, where it is eliminated in urine. Thus, urea is an important parameter for testing kidney and liver function. Urine and blood serum have normal urea concentrations in the range of 2.7 to 7.5 mM [26]. High concentrations of urea in body fluid can cause diseases such as kidney failure, urinary tract obstruction, or gastrointestinal blood loss while lower concentrations can lead to hepatic malfunction, cachexia, or nephritic disorder [27]. Therefore, it is important to precisely measure urea concentration in body fluid to monitor health. In this study, we propose an electrochemical system to detect urea using the LMP91000 IC with a Co-based metal catalyst. The system can read data from functionalized electrodes through its measuring circuit before being transferred to a PC for processing and analysis. An algorithm is built to process the obtained signal and compare it to the results from a commercial device to evaluate the algorithm's performance. The system is not only capable of detecting urea but can also be customized to detect other chemicals.

2. System design and experimental setup

2.1. Materials and components

An LMP91000EVN sensor was utilized as a miniaturised electrochemical measuring system and was purchased from Texas Instruments (USA). An Arduino UNO R3 KIT (Arduino.cc) was used as the micro-controller for the system to communicate with the measuring circuit and PC. Commercial electrodes were purchased from Biodevice Technology, Ltd. (Japan) for system evaluation. All chemicals were purchased from Sigma Aldrich, namely, polyvinyl pyrroidone K30, thioacetamide, cobalt (II) acetate, Nafion, potassium hydroxide (KOH), urea, and potassium chloride (KCl). A compact potentiostat, namely, the BDTminiSTAT100 from Biodevice Technology, Ltd. (Japan), was used to compare the performance of the system.

2.2. System design

The system includes three main blocks: the electrodes, electrochemical measuring circuit, and data acquisition. There are three electrodes used for performing electrochemical measurements i.e., the working, counter, reference electrodes. The working electrode was made of copper and fabricated by circuit board printing. After fabrication, this electrode was processed so that chemicals could be attached to it for urea detection. The counter electrode was made of platinum to ensure that its surface was not affected by the chemical reactions in the experiments. The final electrode is the reference electrode, which was a type of standard reference electrode with a stable and well-known electrode potential.

In this report, cyclic voltammetry measurements with a three-electrode system were used as the standard method for urea detection. An output voltage was generated by the LMP91000 proportional to the current flowing through the working electrode. The trans-impedance amplifier (TIA) provided the output voltage at the output stage. It converts the current flowing from the working electrode to the counter electrode into a voltage at a directly proportional rate as shown in the schematic diagram of the LMP91000 in Fig. 1A. To perform the desired measurements, some hardware configurations were performed manually (Fig. 1B) including the J_MENB jumper configured to enable manual operation mode. In manual mode, the Enable Module of the LMP91000 was tied to GND, which allows users to set function parameters such as TIA Control and RLOAD. While TIA Control changes the gain of trans-impedance amplifier, RLOAD is used to adjust the value of the current drawn from the sensor to the TIA during measurements. In our system, the TIA Control and the RLOAD were set with values of 3.5 kΩ and 10 Ω, respectively. Additionally, the R6 resistor was removed to connect an external reference voltage of 3.3 V between the VREF and GND test points instead of the default internal reference voltage of 2.5 V. This helps the output voltage of the board to reach 2.2 V if the internal zero parameter is assigned to be 67% of the reference voltage. In addition, the two-wire jumper was removed to activate three-electrode (working, counter, and reference) CV measurements for a portable potentiostat system.

To configure other parameters and receive data from the electrodes, an Arduino UNO R3 KIT was used as the central processing unit (CPU) of the system. The Arduino powers and communicates to the LMP91000 through I2C standard communication. The Arduino KIT and LMP91000 module were stacked to minimize the size of the device, as shown in Fig. 1B. The Arduino KIT was placed at the bottom of the stack and connected to the LMP91000 module. In addition

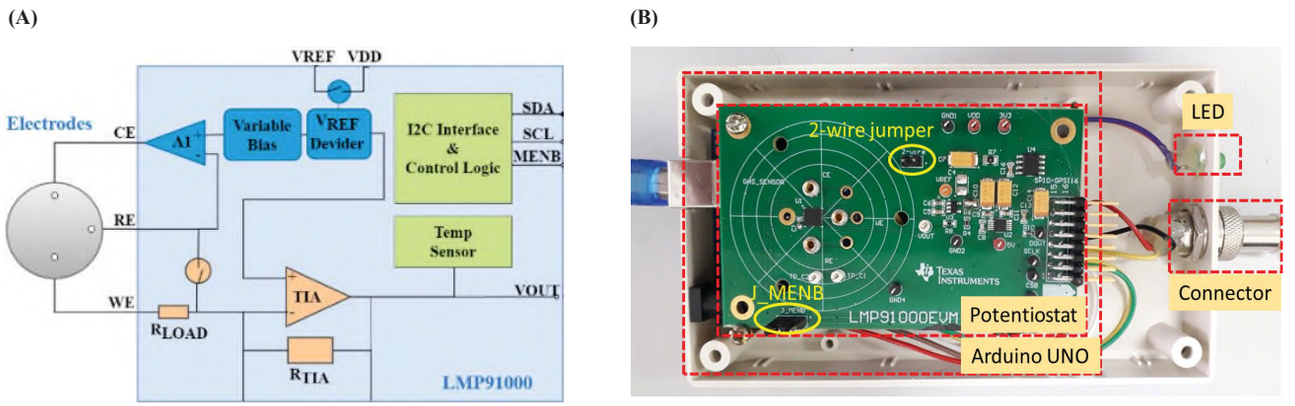

Fig. 1. (A) Block diagram of LMP91000 IC; (B) Image of the proposed system after assembly.

to the I2C connection, the output voltage of the LMP91000 (VOUT) was wired to the analogue input of the Arduino module (A0). A graphical user interface on the computer was developed using MATLAB software to receive and display the obtained data through a communication port (COM). The software plots the data on a graph with different colours for each scan making it is easy for users to observe and evaluate results. The LMP91000 module and Arduino UNO are the two main components of the proposed system. They were purchased from authorized retailers for $131.67 and $27.60, respectively. The cost of the other components was about $15. So, the total cost of the system is estimated to be about $174.27. This number is small compared to the ~$10,000 price tag of commercial device such as the Autolab Potentiostat or BDTminiSTAT100.

2.3. Experimental setup

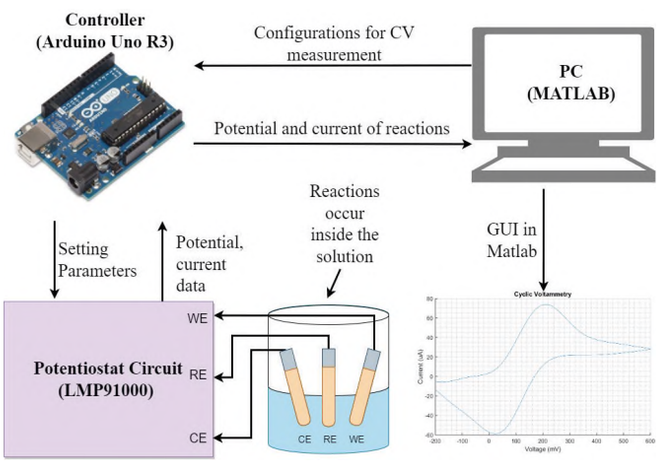

Fig. 2. Experimental setup diagram for urea detection.

The working electrode with a diameter of 10 mm was self-designed as a pad using Altium Designer software and fabricated by printed circuit board technology (PCB). The working electrode surface was then cleaned and functionalized by CoS materials according to a standard process (Fig. 2). Firstly, the copper electrode was cleaned by isopropyl alcohol (IPA) in an ultrasonic vibration tank about 10 minutes before being dried by pure nitrogen gas. Secondly, the CoS solution was made by adding 3 mg CoS into a solution including 1.6 ml distilled water, 0.4 ml ethanol, and 20 µl Nafion. Then, this mixture was placed in an ultrasonic vibration tank for 10 min to achieve a homogeneous solution. Finally, the CoS solution was dropped onto the copper electrode surface and dried under room temperature conditions. Following this, the three-electrode system was immersed in a solution with different urea concentrations. CV electrochemical measurements were made to investigate the change of the urea through an electrical signal. Some parameters were configured on software, including the potential range from -0.2 to 0.6 V, scan rate at 20 mV/s, and sample rate at 50 Hz.

3. Results and discussion

3.1. Signal processing algorithm

After assembly, the proposed system was tested with a standard redox solution containing Fe(II)/Fe(III) 5 mM and KCl 0.1 mM to evaluate system performance and make comparisons to the commercial potentiostat BDTminiSTAT100 (Biodevice Technology, Japan). Three electrodes were immersed in the redox solution and the measurement parameters were configured on the software with potential range from -0.2 to 0.6 V, scan rate at 10 mV/s, and sample rate at 50 Hz. The results show that the obtained signal had a standard duck-shaped CV plot as shown in Fig. 3A. However, the signal had some high frequency noise because it was raw data without any processing. Because the results will not be reliable with noisy data, a signal processing algorithm was developed as shown in Algorithm 1. Firstly, the software is connected to the Arduino KIT through COM port at the baud rate of 9600 bps and some function parameters were set to configure the system for CV measurements. After

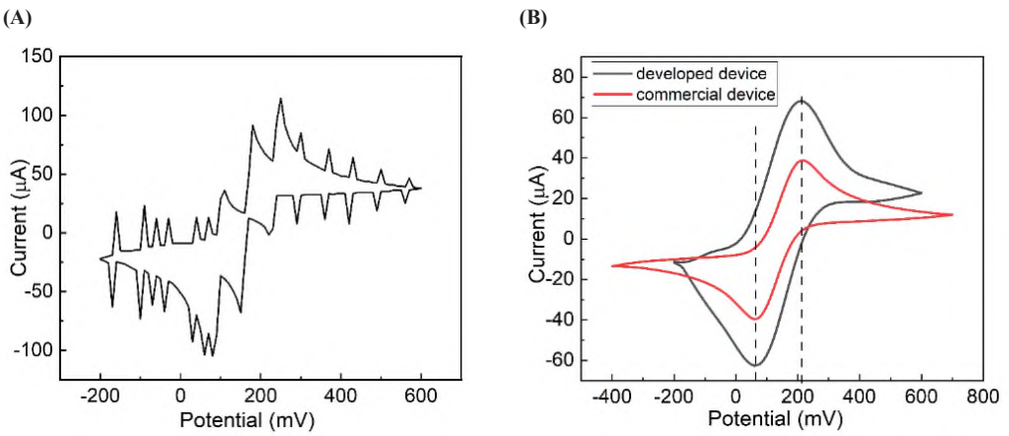

Fig. 3. Signal processing. (A) The initial signal from the proposed system with noise. **(B)** The signal after being processed compared to the signal from a commercial device.

Algorithm 1. Firmware for data acquisition.	
1	Begin serial communication at 9600 bps
2	Set function parameters: starting and ending voltages, step and cycle
3	Initialize the data array
4	While (i < ((ending voltage – starting voltage)/step +1)*cycle*2)
5	Take samples with ADC available on Arduino KIT
6	Convert and save samples into the data array
7	End While
8	Convert the data to the frequency domain using FFT
9	Apply low-pass filter with a cut-off frequency of 2 Hz
10	Convert the data back to the time domain using inverse fast fourier transform
11	Display the signal

configuration, the system carried out sampling through an analogue-to-digital converter (ADC) available on the Arduino KIT and transferred the data to PC. The obtained voltage data were converted into current and saved into a data array, which was initialized until the array contained a number of elements equal to ((ending voltage - starting voltage)/step +1)*cycle*2. Following this, the data was passed through a low-pass filter with a cut-off frequency of 2 Hz. This cut-off frequency was determined based on the conversion of the signal into the frequency domain using a fast fourier transform (FFT). Finally, the processed signal was displayed on a graph, e.g., the black line in Fig. 3B.

The results show the high-frequency noise was removed from the signal and thus significantly smoothed. The obtained signal had the standard duck shape, a characteristic of CV measurements with a redox solution. The same experiment was also performed with a commercial potentiostat from Bio Device Tech. The settings (scan rate, sample rate) were kept the same for both devices. The current signal from the device is displayed as the red line in Fig. 3B. It is clear that both data are similar in shape and have similar positions of oxidation and reduction peaks. The oxidation peaks appear at 200 mV, while the reduction peaks appear at 80 mV. There is a difference in current amplitude between the two signals because of the circuit resistor. The results show that the proposed algorithm helped the system operate like a commercial potentiostats and the obtained signal clearly exhibited the redox process of the solution. Besides, there are many advantages of the obtained signal from the proposed system compared to similar systems developed by other research groups [23-25] in terms of the shape of the signal and accuracy.

3.2. Electrochemical detection of urea

The three-electrode system was immersed in solutions with different urea concentrations. CV measurements were taken during each experiment to monitor the change of the current as it flowed through the liquid sample as the voltage value shifted. The results show that a signal peak began to appear when urea was in the sample and the value of the current peak increased considerably with increasing urea concentration as shown in Fig. 4A. This can be explained that urea was oxidized by KOH on the electrode surface of the CoS catalyst following a direct oxidation mechanism as shown in Eqs. (1)-(3) [28]:

At the anode:

$$CoS+OH^- \rightarrow CoSOH+ e^- \quad (1)$$

$$CO(NH_2)_2+6OH^- \rightarrow N_2+5H_2O+ CO_2+6e^- \quad (2)$$

At the cathode:

$$6H_2O+6e^- \rightarrow 3H_2+6OH^- \quad (3)$$

In Eq. (1), CoS was electrochemically oxidized to CoSOH, which participated in the urea oxidation reaction as a catalyst. Then, urea was oxidized by KOH

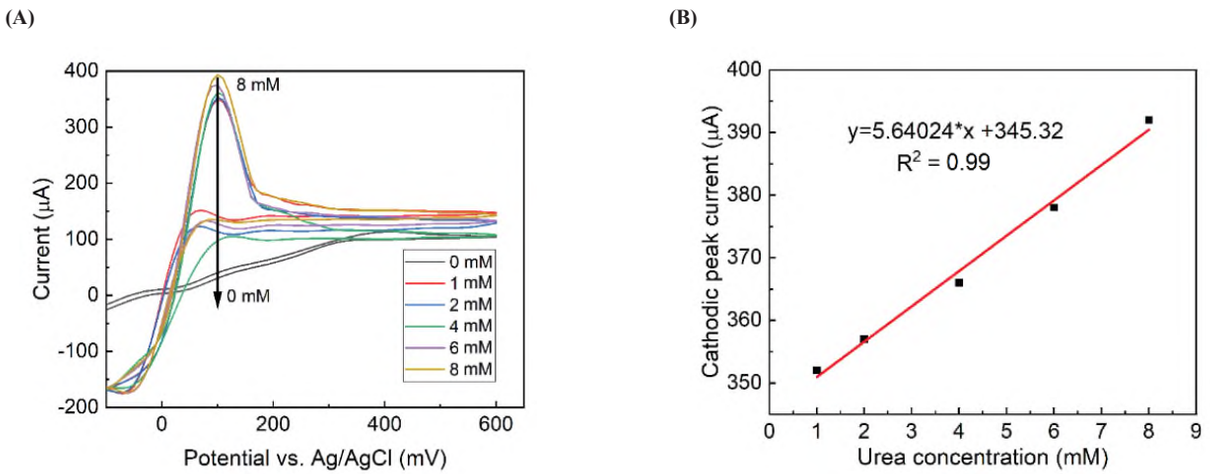

Fig. 4. (A) The electrochemical signal obtained from the proposed system with different urea concentrations; (B) Linear calibration line plotted between the magnitude of response current and urea concentration using the proposed system.

to release electrons, N_2, and CO_2 as shown in Eq. (2). So, more electrons were generated or the current response increased when the urea concentration changed from 1 mM to 8 mM. A linear trendline was fit to the relationship between the magnitude of the current response and urea concentration. The equation of best fit was $I_{response\ current}$ (μA) = 5.64024*urea concentration (mM) + 345.32, as shown Fig. 4B. From this linear relation, it is easy to determine the urea concentration through the current response.

A comparison between these results and results from other urea detection publications using non-enzymatic methods was performed as shown in Table 1. As can be seen, the CoS-based electrodes were more sensitive than Co-MOF. Notably, the working potential in this study was the lowest.

Table 1. Comparative data for electrochemical urea detection.

Electrodes	Electrolyte	Potential (V)	Sensitivity (μAmM^{-1})	Ref.
$NiCo_2O_4$	0.1 M NaOH	0.5	8.2	[29]
Co-MOF	0.1 M KOH	0.45	5	[30]
HEA: Graphene composite	1 M KOH	0.3	37.4	[31]
SnO_2	1 M KOH	0.65	18	[32]
CoS	0.1 M KOH	0.1	7.13	This work

4. Conclusions

In this work, a miniaturised potentiostat system using an LMP91000 analogue front-end was developed to detect urea concentration in solution. The system included three main blocks: the electrodes, the electrochemical measuring circuit, and data acquisition. The data was read from three-electrode system and transferred to PC through a COM port. An algorithm was developed to process the signal before display on the graphic user interface. The system was then tested with a standard redox solution and compared to a commercial potentiostat to evaluate the performance of the signal processing algorithm and the system in general. The results show that the obtained signals from the proposed system and the commercial potentiostat device are similar. The data clearly exhibit the redox process of the solution with oxidation and reduction peaks. Additionally, the system was used to detect urea in the solution. The working electrode surface was functionalized to attach CoS particles to it. The efficiency of the surface functionality process was confirmed by optical measurements. The results show that the system could detect and quantify urea concentration by CV measurements. Urea concentration was found to be proportional to the oxidation current peak by a first order function. Besides, the effect of scan rate on the signal and the selectivity of the proposed system were also investigated. The results show that the oxidation peak current increased linearly with the increase of the scan rate and that the electrodes have high selectivity with urea. With these achieved results, the proposed system not only demonstrated its potential in urea detection but also showed the ability to detect some other toxic substances such as nitrate or pesticides.

CRediT author statement

Chi Tran Nhu: Experiment, Writing, Review; Phu Nguyen Dang: Conceptualization, Measurement, Data analyst, Editing; Tung Bui Thanh: Writing, Editing, Data analyst; Trinh Chu Duc: Review, Data analyst, Editing.

ACKNOWLEDGEMENTS

This work has been supported by VNU University of Engineering and Technology under project number CN21.17.

COMPETING INTERESTS

The authors declare that there is no conflict of interest regarding the publication of this article.

REFERENCES

[1] Y. Huang, et al. (2017), "Disease-related detection with electrochemical biosensors: A review", *Sensors (Switzerland)*, **17(10)**, DOI: 10.3390/s17102375.

[2] N.J. Ronkainen, et al. (2010), "Electrochemical biosensors", *Chem. Soc. Rev.*, **39(5)**, pp.1747-1763.

[3] http://spie.org/Publications/Book/784938.

[4] W. Jia, et al. (2013), "Electrochemical tattoo biosensors for real-time noninvasive lactate monitoring in human perspiration", *Analytical Chemistry*, **85(14)**, pp.6553-6560.

[5] W. Gao, et al. (2016), "Fully integrated wearable sensor arrays for multiplexed in situ perspiration analysis", *Nature*, **529**, pp.509-514.

[6] A.J. Bandodkar, et al. (2014), "Epidermal tattoo potentiometric sodium sensors with wireless signal transduction for continuous non-invasive sweat monitoring", *Biosens. Bioelectron.*, **54**, pp.603-609.

[7] B. Schazmann, et al. (2010), "A wearable electrochemical sensor for the real-time measurement of sweat sodium concentration", *Analytical Methods*, **2(4)**, pp.342-348.

[8] B.R. Baker, et al. (2006), "An electronic, aptamer-based small-molecule sensor for the rapid, label-free detection of cocaine in adulterated samples and biological fluids", *J. Am. Chem. Soc.*, **128(10)**, pp.3138-3139.

[9] J.L. He, et al. (2011), "Electrochemical aptameric sensor based on the Klenow fragment polymerase reaction for cocaine detection", *Biosens. Bioelectron.*, **26(10)**, pp.4222-4226.

[10] S. Rauf, et al., "Label-free nanopore biosensor for rapid and highly sensitive cocaine detection in complex biological fluids", *ACS Sensors*, **2(2)**, pp.227-234.

[11] J. Kim, et al. (2016), "Noninvasive alcohol monitoring using a wearable tattoo-based iontophoretic-biosensing system", *ACS Sensors*, **1(8)**, pp.1011-1019.

[12] A.S. Campbell, et al. (2018), "Wearable electrochemical alcohol biosensors", *Curr. Opin. Electrochem.*, **10**, pp.126-135.

[13] C. Chen, et al. (2013), "Recent advances in electrochemical glucose biosensors: A review", *RSC Adv.*, **3(14)**, pp.4473-4491.

[14] J. Wang (2008), "Electrochemical glucose biosensors", *Chem. Rev.*, **108(2)**, pp.814-825.

[15] N.J. Ronkainen, et al. (2010), "Electrochemical biosensors", *Chem. Soc. Rev.*, **39(5)**, pp.1747-1763.

[16] A. Benvidi, et al. (2015), "A highly sensitive and selective electrochemical DNA biosensor to diagnose breast cancer", *J. Electroanal. Chem.*, **750**, pp.57-64.

[17] H.A. Rafiee-Pour, et al. (2016), "A novel label-free electrochemical miRNA biosensor using methylene blue as redox indicator: Application to breast cancer biomarker miRNA-21", *Biosens. Bioelectron.*, **77**, pp.202-207.

[18] P.Y. Lin, et al. (2012), "Detection of alpha-methylacyl-CoA racemase (AMACR), a biomarker of prostate cancer, in patient blood samples using a nanoparticle electrochemical biosensor", *Biosensors*, **2(4)**, pp.377-387.

[19] A. de la Escosura-Muñiz, et al. (2010), "Gold nanoparticle-based electrochemical magnetoimmunosensor for rapid detection of anti-hepatitis B virus antibodies in human serum", *Biosens. Bioelectron.*, **26(4)**, pp.1710-1714.

[20] M.D.M. Dryden, A.R. Wheeler (2015), "DStat: A versatile, open-source potentiostat for electroanalysis and integration", *PLOS ONE*, **10(10)**, DOI: 10.1371/JOURNAL.PONE.0140349.

[21] V. Bianchi, et al. (2020), "A wi-fi cloud-based portable potentiostat for electrochemical biosensors", *IEEE Trans. Instrum. Meas.*, **69(6)**, pp.3232-3240.

[22] S.V. Raj, et al. (2018), "Fabrication of a configurable multi-potentiostat for LOC applications", *Mater. Today Proc.*, **5(8)**, pp.16732-16739.

[23] A.R. Baranwal, et al. (2021), "Development of completely automated poly potential portable potentiostat", *ECS J. Solid State Sci. Technol.*, **10(2)**, DOI: 10.1149/2162-8777/abdc15.

[24] O.S. Hoilett, et al. (2020), "Kickstat: A coin-sized potentiostat for high-resolution electrochemical analysis", *Sensors (Switzerland)*, **20(8)**, pp.1-12.

[25] A.F.D. Cruz, et al. (2014), "A low-cost miniaturised potentiostat for point-of-care diagnosis", *Biosens. Bioelectron.*, **62**, pp.249-254.

[26] D. Dutta, et al. (2014), "SnO_2 quantum dots-reduced graphene oxide composite for enzyme-free ultrasensitive electrochemical detection of urea", *Analytical Chemistry,* **86(12)**, pp.5914-5921.

[27] A. Sharma, et al. (2017), "Studies on clay-gelatin nanocomposite as urea sensor", *Appl. Clay Sci.*, **146**, pp.297-305.

[28] J. Jiang, et al. (2019), "One-step synthesis of nickel cobalt sulfide nanostructure for high-performance supercapacitor", *J. Mater. Sci.*, **54(18)**, pp.11936-11950.

[29] C. Bao, et al. (2019), "Ultrathin nickel-metal–organic framework nanobelt based electrochemical sensor for the determination of urea in human body fluids", *RSC Adv.*, **9(50)**, pp.29474-29481.

[30] X. Wang, et al. (2021), "Conductive 2D metal-organic framework (Co, NiCo, Ni) nanosheets for enhanced non-enzymatic detection of urea", *Electroanalysis*, **33(6)**, pp.1484-1490.

[31] R. Ashwini, et al. (2022), "Optimization of NiFeCrCoCu high entropy alloy nanoparticle - graphene (HEA-G) composite for the enhanced electrochemical sensitivity towards urea oxidation", *J. Alloys Compd.*, **903**, DOI: 10.1016/J.JALLCOM.2022.163846.

[32] S.G. Ansari, et al. (2015), "Electrochemical enzyme-less urea sensor based on nano-tin oxide synthesized by hydrothermal technique", *Chem. Biol. Interact.*, **242**, pp.45-49.